agronomy

MDPI

Article

High-Performance Liquid Chromatography–Quadrupole Time-of-Flight Tandem Mass Spectrometry-Based Profiling Reveals Anthocyanin Profile Alterations in Berries of Hybrid Muscadine Variety FLH 13-11 in Two Continuous Cropping Seasons

Seyit Yuzuak [1,3], James Ballington [2], Gui Li [1,†] and De-Yu Xie [1,*]

[1] Department of Plant and Microbial Biology, North Carolina State University, Raleigh, NC 27695-7612, USA; sytyzk@gmail.com (S.Y.); ligui@hnlky.cn (G.L.)
[2] Department of Horticultural Sciences, North Carolina State University, Raleigh, NC 27695-7609, USA; jim_ballington@ncsu.edu
[3] Department of Molecular Biology and Genetic, Burdur Mehmet Akif Ersoy University, Burdur 15200, Turkey
* Correspondence: dxie@ncsu.edu
† Current address: Department of Forest and Grass Breeding, Hunan Academy of Forestry, Changsha 410004, China.

Abstract: FLH 13-11 is an F1 interspecific hybrid muscadine grape genotype that was developed to produce new anthocyanins for pigment color stability. This hybrid resulted from a cross between 'Marsh' (*Vitis munsoniana*) and 'Magoon' (*V. rotundifolia*) and has been cultivated for the wine and juice industry. This report characterizes anthocyanins produced in fully ripe berries and reveals a significant difference in total anthocyanin contents from two continuous cropping seasons. High-performance liquid chromatography with a diode array detector (HPLC-DAD) and HPLC–quadrupole time-of-flight tandem mass spectrometry (HPLC-qTOF-MS/MS) were used to profile anthocyanins in berries. The resulting data showed that fourteen anthocyanins were detected, six from 2011 and nine from 2012, with only one produced in both seasons. However, the anthocyanidin profiles of the berries were the same. Five anthocyanins were annotated as diglucosides of anthocyanidins based on MS/MS features, including delphinidin 3,5-diglucoside produced in both seasons, cyanidin 3,5-diglucoside mainly formed in 2011, petunidin 3,5-diglucoside, malvidin 3,5-diglucoside, and peonidin 3,5-glucoside only detected in 2012. Also, three anthocyanidin-diglucoside-like anthocyanins and three monoglucosides, including peonidin 3-glucoside, delphinidin 3-glucoside like, and pelargonidin 3-glucoside-like anthocyanins, were detected in 2011 and 2012, respectively. These results indicate that FLH 13-11 can produce both anthocyanidin-diglucosides and -monoglucosides, and their biosynthesis is closely dependent on cropping years.

Keywords: anthocyanidins; anthocyanidin-3,5-O-diglucoside; anthocyanidin-3,5-O-monoglucoside; anthocyanins; HPLC–quadrupole time-of-flight tandem mass spectrometer; *Vitis rotundifolia*; metabolic profiling

Citation: Yuzuak, S.; Ballington, J.; Li, G.; Xie, D.-Y. High-Performance Liquid Chromatography–Quadrupole Time-of-Flight Tandem Mass Spectrometry-Based Profiling Reveals Anthocyanin Profile Alterations in Berries of Hybrid Muscadine Variety FLH 13-11 in Two Continuous Cropping Seasons. *Agronomy* **2024**, *14*, 442. https://doi.org/10.3390/agronomy14030442

Academic Editor: Enrico Porceddu

Received: 30 January 2024
Revised: 14 February 2024
Accepted: 20 February 2024
Published: 24 February 2024

1. Introduction

Muscadine (*Vitis rotundifolia* Michx) is a grape crop native to the south-eastern and south-central regions of the United States [1]. To date, this crop is mainly produced commercially in Florida, Georgia, Alabama, Louisiana, South Carolina, Mississippi, and North Carolina [2]. Many years of breeding efforts have created multiple superior cultivars for the fresh market, wine, and unfermented juice industries [3].

FLH 13-11 is an interspecific muscadine F_1 hybrid that resulted from the cross of 'Marsh' × 'Magoon' made by the grape breeding program of the University of Florida,

located in Leesburg, Florida. 'Marsh' is a wild selection of *Vitis munsoniana*, and 'Magoon' is a *V. rotundifolia* cultivar that resulted from the cross of 'Thomas' × 'Burgaw'. The FLH 13-11 muscadine variety is being cropped at the Castle Hayne research station in Wilmington, North Carolina (NC). Wilmington has a humid subtropical climate. According to the National Weather Service Wilmington, in contrast to the very cold winters of 2009–2010, the winters of 2011 and 2012 consistently had above-normal temperatures. In 2011, the average temperatures were above normal from winter through summer, while in 2012, temperatures were consistently above normal from January through July, resulting in moderate to severe droughts. July 2012 was the hottest month on record since temperature records began in 1874. Therefore, 2012 was the 11th warmest year on record for Wilmington's climate [https://www.weather.gov/ilm/ClimateSummary, accessed on 23 June 2018]. Castle Hayne is located in New Hanover County, NC, USA, and is part of Wilmington (longitude, −77.9; latitude, 34.36 DD (Decimal Degrees); and altitude, 16 ft.). The average high temperature in Castle Hayne was reported as 76.5 F (24.7 °C) and 76 F (24.4 °C) for 2011 and 2012, but the average annual maximum high temperatures were 89.2 F (31.7 °C) and 88.2 F (31.2 °C) for 2011 and 2012 (Figure S14). This shows that although there was no significant difference in the average temperature between the two consecutive years, the average of the annual maximum high temperatures in the region was considerably higher than the average temperature of that year. A similar situation applies to the Wilmington area where Castle Hayne is located. The average high temperature in Wilmington was reported as 75.2 F (24 °C) and 75.1 F (23.9 °C) for 2011 and 2012, but the average annual maximum high temperatures were 102 F (38.8 °C) and 103 F (39.4 °C) for 2011 and 2012 (Figure S13) [https://www.weather.gov/ilm/ClimateSummary, accessed on 23 June 2018].

Anthocyanins are the main active nutraceuticals in muscadine berries, which provide antioxidative and other health values [4–7]. To date, anthocyanins have been analyzed in intensive studies in a number of muscadine cultivars. The first anthocyanin molecule isolated from muscadine berries of the Hunt cultivar was named muscadinin (3,5-diglycosidyl-3′-O-methyldelphinidin, namely petunidin 3, 5-diglucoside) by W.L. Brown in 1940 [1]. The main anthocyanins were then identified from berries and other tissues [8–13]. The most common muscadine anthocyanidins are delphinidin, malvidin, petunidin, cyanidin, pelargonidin, and peonidin (Figure 1).

The most common anthocyanins are non-acylated 3,5 diglucosides of delphinidin, malvidin, petunidin, cyanidin, pelargonidin, and peonidin, which have been extracted from fresh fruits of Noble, Tarheel, and other cultivars [9,11,12,14,15]. The contents of these six anthocyanins in muscadine berries vary widely among cultivars. More importantly, the abundance of each of the six anthocyanins has been demonstrated to control wine and juice color. For example, high-quality wine color was found to relate to high amounts and percentages of malvidin 3,5-diglucoside but low amounts and percentages of delphinidin 3,5-diglucoside and cyanidin 3,5-diglucoside [9]. Wine production research has shown that muscadine varieties with high amounts of cyanidin 3,5-diglucoside produce the poorest wine color and color stability [9]. Given that malvidin 3,5-diglucoside is structurally featured with two methyl groups in the B-ring, there is a general assumption that the degree of methylation of each aglycone is associated with the pigment stability of muscadine wine [9].

However, maintaining pigment stability remains a challenging problem with muscadine wine and juice products [12,16]. To address this problem, both intraspecific and interspecific muscadine hybrids have been generated to attempt to produce new genotypes with more color-stable anthocyanin pigment ratios [12,17–19]. These studies have achieved progress in not only improving anthocyanin ratios of methylated to non-methylated ones, but also producing additional muscadine anthocyanins. For example, 25 anthocyanins including 5 common anthocyanidin-3,5-diglucosides and new anthocyanins were identified in 14 black muscadine hybrids [17]. Although pelargonidin and its monoglucoside and diglucoside have not been reported from common commercial verities such as Noble and Nesbitt, these metabolites were observed in hybrids. These results demonstrated that

conventional breeding methods can produce genotypes with improved anthocyanin ratios and new anthocyanins for the color quality improvement of wine and juice products. Therefore, the goal of this study was to use HPLC-qTOF-MS/MS technology to determine the anthocyanin profile and structure in berries of the FLH 13-11 hybrid muscadine genotype.

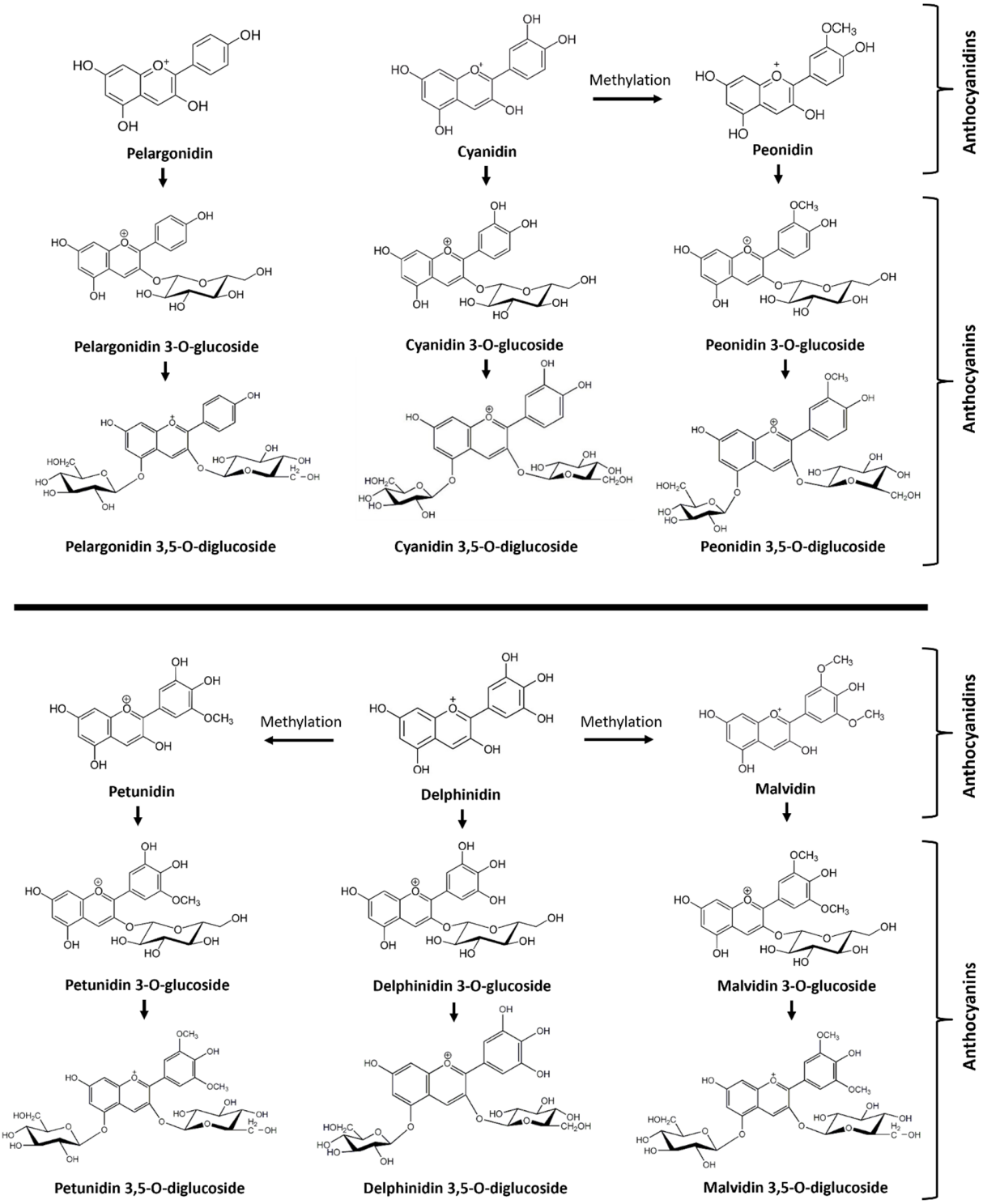

Figure 1. Overview of anthocyanidins and anthocyanins identified in berries of different muscadine varieties. Six anthocyanidins include pelargonidin, cyanidin, delphinidin, peonidin, petunidin, and malvidin. Anthocyanins include six monoglucosides of anthocyanidins and six diglucosides of anthocyanidins.

2. Materials and Methods

Chemical agents. Peonidin 3-O-glucoside (≥97%, HPLC grade, cat# 42008), cyanidin 3,5-diglucoside (≥90%, HPLC grade, cat# 74397), pelargonidin chloride (HPLC grade, cat# P1659), and cyanidin chloride (≥95%, HPLC grade, cat# 79457) were purchased from Sigma-Aldrich® (St Louis, MO, USA). Delphinidin chloride (≥95%, HPLC grade, cat# 43725) was purchased from Fluka™ Chemical (Ronkonkoma, NY, USA). Hydrochloric acid (36.5–38%) was purchased from BDH (cat#: BHH3028-2.5L, West Chester, PA, USA). Acetonitrile (LC-MS grade, cat#: 9829-03), glacial acetic acid (HPLC grade, cat#: 9515-03), and methanol (LC-MS grade, cat#: 9830-03) were purchased from Avantor® (Center Valley, PA, USA). Ethyl alcohol, 200 proof (cat#: EX0276-1) was purchased from EMD (Burlington, MA, USA).

Plant material. FLH 13-11 vines were grown at the Castle Hayne Station in Wilmington, North Carolina. Berries were fully ripened in the first two weeks of September each year. Berries were collected on 6 September 2011 and 10 September 2012. Fruits were harvested and immediately placed on ice in a cooler and transported to the laboratory. All fresh berries were frozen in liquid nitrogen and then stored in −80 °C freezers. Frozen berries were ground to fine powder in liquid nitrogen using a steel blender. Powdered samples were completely dried via lyophilization from −40 °C to −20 °C for 72 h. Dried powder samples were stored at −80 °C until the extraction of anthocyanins, as described below.

Extraction and measurement of anthocyanins. First, 100 mg of freeze-dried berry powder was suspended in 1.0 mL of extraction buffer, which was composed of 0.5% HCl in methanol: dH_2O (50:50, *v*/*v*) in a 2 mL Eppendorf tube at room temperature. The tube was vigorously vortexed for 45 s, sonicated for 10 min, and then centrifuged at 10,000 rpm for 10 min. The supernatant was transferred into a new 1.5 mL tube. This step was repeated using 0.5 mL of extraction buffer. The two extractions were pooled together in the 1.5 mL tube. To remove chlorophyll and non-polar lipids in the extraction, the 1.5 mL ethanol/water extraction was mixed with 0.5 mL of chloroform in a 2 mL tube. The mixture was vortexed vigorously for 45 s and centrifuged at the speed of 10,000 rpm for 5 min. The resulting upper ethanol–water phase (about 750 µL) containing red pigment was pipetted into a new 1.5 mL tube. The bottom chloroform phase containing chlorophyll and non-polar lipids was disposed of into a waste container. This step was repeated once. The resulting upper red phase was stored at −20 °C for anthocyanin analysis described below. Three replications were included for varieties in this experiment.

The absorbance (ABS) of ethanol–water phase extracts was recorded at the wavelength of 530 nm on a HEλIOSγ UV–Visible spectrophotometer. The extraction buffer was used as a blank control. A 10 µL extract was added to 990 µL of extraction buffer to dilute anthocyanin concentrations to measure the ABS value. Authentic standard peonidin 3-O-glucoside was used to establish a standard curve. The total anthocyanin content in berries was estimated as a peonidin 3-O-glucoside equivalent (µg/g) according to the standard curve.

After the measurement of total anthocyanin contents for each sample, 720 µL of ethanol–water anthocyanin extract was dried off using a SpeedVac Concentrator connected to a Refrigerated Condensation Trap for 2 h. The remaining pellet was dissolved in 720 µL of 0.1% HCl in methanol 100% in a 1.5 mL tube. The tube was centrifuged at 10,000 rpm for 10 min. The resulting clear supernatant was transferred to a new 1.5 mL tube and then stored at −20 °C for anthocyanin analysis. Then, 200 µL of HCl–methanol extract for each sample was transferred to a glass insert, which was placed in a 1.5 mL glass vial for HPLC and HPLC-qTOF-MS/MS analysis, described below. A 50 µL HCl–methanol extract was used for hydrolysis.

Hydrolysis of anthocyanins. The hydrolysis of anthocyanins followed our protocol reported previously [20]. In brief, 50 µL of anthocyanin extract was added into 450 µL of an *n*-butanol/HCl (95:5, *v*/*v*) solvent contained in a 1.5 mL tube. This mixture was boiled for 1 h. After the sample was cooled down to room temperature, it was dried off with flow nitrogen gas. The remaining residue was suspended in 200 µL of 0.1% HCl–methanol. The

sample was centrifuged at 12,000 rpm for 10 min. The supernatant was transferred to a new 1.5 mL tube and stored at −20 °C for anthocyanidin analysis. A 200 µL HCl–methanol extract for each sample was transferred to a glass insert, which was placed in a 1.5 mL glass vial for HPLC and LC-MS/MS analysis, described below.

High performance liquid chromatography–diode array detector analysis. Anthocyanins profiling was carried out using the high-performance liquid chromatography–diode array detector (HPLC-DAD) technique on a 2010 eV LC instrument (Shimadzu, Kyoto, Japan) as reported previously [20,21]. Both anthocyanidins and anthocyanins were separated on an analytical column of Eclipse XDB-C18 (250 mm × 4.6 mm, 5 µm, Agilent, Santa Clara, CA, USA), as also reported previously [21]. The mobile phase solvents were composed of 1% acetic acid in water (solvent A: 1% HPLC-grade acetic acid in LC-MS-grade water) and 100% acetonitrile (solvent B) (LC-MS grade). The column was equilibrated for 30 min using solvent A/B (80:20). Then, a gradient solvent system was developed to separate metabolites. It was composed of ratios of solvent A to B: 80:20 (0–5 min), 80:20 to 70:30 (5–10 min), 70:30 to 65:35 (10–20 min), 65:35 to 60:40 (20–30 min), 60:40 to 55:45 (30–40 min), 55:45 to 50:50 (40–45 min), 50:50 to 48:52 (45–50 min), 48:52 to 45:55 (50–55 min), 45:55 to 40:60 (55–58 min), 40:60 to 10:90 (58–58.5 min), and 10:90 to 80:20 (58.5–60 min). After these gradient steps, the column was equilibrated and washed with solvent A/B (80:20) for 10 min. The flow rate was 0.4 mL/min and the injection volume was 20 µL. The UV spectrum was recorded from 190 to 800 nm. Pelargonidin chloride, cyanidin chloride, delphinidin chloride, and peonidin 3-glucoside were used as authentic standard controls.

HPLC–quadrupole time-of-flight-tandem mass spectrometer (HPLC-qTOF-MS/MS) analysis. HPLC-TOF-MS/MS analysis was performed on an Agilent Technologies (Santa Clara, CA, USA) 6210 time-of-flight LC-MS/MS, as reported previously [22]. The mobile phase solvents were composed of 1% acetic acid in water (solvent A: 1% HPLC-grade acetic acid in LC-MS-grade water) and 100% acetonitrile (solvent B) (LC-MS grade), which formed another gradient solvent system to separate anthocyanins and anthocyanidins for the LC/MS/MS assay. A gradient solvent system was composed of gradient ratios of solvent A to B: 85:15 (0–10 min), 85:15 to 80:20 (10–20 min), 80:20 to 75:25 (20–30 min), 75:25 to 65:35 (30–35 min), 65:35 to 60:40 (35–40 min), 60:40 to 50:50 (40–55 min), 50:50 to 10:90 (55–60 min), and 10:90 to 90:10 (60–70 min). After the last gradient step, the column was equilibrated and washed for 10 min with solvents A/B (85:15). The flow rate was 0.4 mL/min. The injection volume of samples was 5.0 µL. The drying gas flow was set to 12 l/min, and the nebulizer pressure was set to 50 psi. As in our recent report using an optimized protocol for anthocyanin ionization [22], a negative mode was used for ionization. The mass spectrum was scanned from 100 to 3000 m/z. The acquisition rate was three spectra per second. Other parameters included fragmentor: 150 v; skimmer: 65 v; OCT 1 RF Vpp: 750 v; and collision energy: 30. In addition, the UV spectrum was recorded from 190 to 600 nm. Pelargonidin chloride, cyanidin chloride, delphinidin chloride, and peonidin 3-glucoside were used as authentic standard controls.

Structure annotation. Anthocyanidin and anthocyanin structure annotation was performed using Agilent MassHunter Software for 6200 Series TOF and 6500 Series G-TOF version B.05.00. To identify anthocyanidins released from the hydrolysis of anthocyanin extracts, the retention time, extracted ion chromatogram (EIC), and mass to charge (m/z) ratio for each peak was analyzed to compare the values with available standards. For those peaks without standards, their EICs and m/z ratios were used for annotation. For each anthocyanin peak detected at 530 nm by HPLC-DAD in two different instruments, their EIC, m/z ratio, finger fragments from CID, and maximum UV spectrum were integrated for structure annotation. Anthocyanin structures reported in the literature were utilized as our references for annotation. If anthocyanin peaks could not match a reported structure, their EIC, m/z, CID fragments, and UV spectrum were provided to show molecular features.

Statistical analysis. Student's t test was performed using Microsoft Excel (2007) to statistically compare contents of total anthocyanins at the $p < 0.05$ significance level. Standard deviation was calculated to reflect variation in contents between biological replicates.

3. Results and Discussion

Total anthocyanin contents in berries. Anthocyanins were measured to compare the effects of two cropping seasons on the total anthocyanin content (TAC) in berries from the field. The resulting data revealed that the contents of anthocyanin were 2.64-fold higher in berries of 2012 than those in 2011 (Figure 2). This result indicates that the production of total anthocyanins is regulated by two different growth seasons. This result is a common phenomenon, given that the biosynthesis of anthocyanins is highly regulated by different environmental conditions. Light conditions and temperatures are two main environmental factors that have been demonstrated to tightly control anthocyanin biosynthesis in plant tissues [20,23–26]. Since there was no significant difference between the annual averages of high temperature and the maximum highest temperature values of 2011 and 2012 in the cultivation area, this finding may suggest that besides temperature, factors such as the intensity of sunlight, wavelengths, polarization degree and direction, humidity, and wind may play a role in the 2.64-fold increase in total anthocyanin content. These factors may also have impacts on the profile of anthocyanin types of the same cultivar growing in two consecutive years.

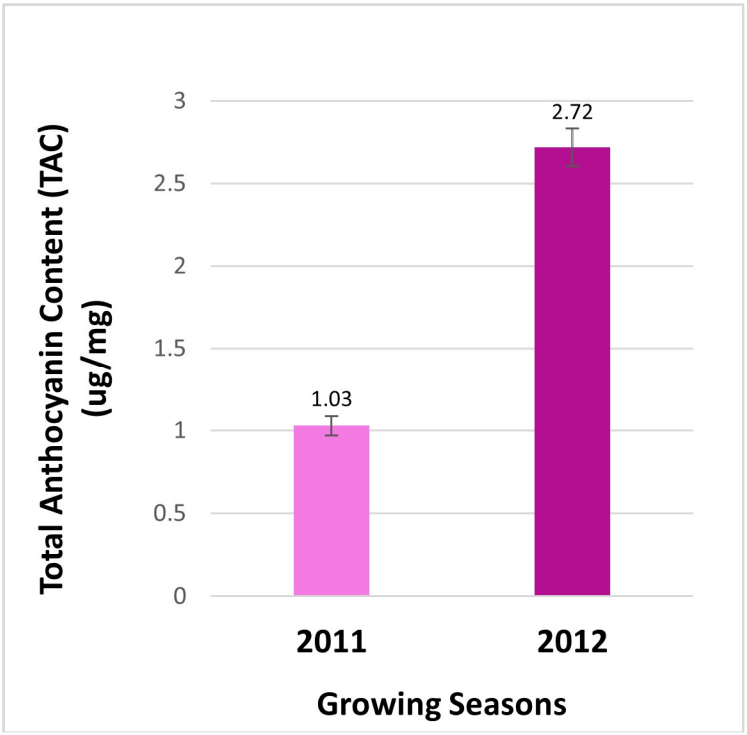

Figure 2. The total anthocyanin contents of extracts from berries of FLH 13-11 collected in the 2011 and 2012 growing seasons.

Alteration of anthocyanin profiles. Anthocyanin profiles were analyzed by HPLC-DAD-based profiling. Chromatographic peaks were recorded at 530 nm to compare anthocyanin profiles in berries between two growth seasons. At least three experimental replicates were performed to understand anthocyanin profiles in berries from the two seasons. The resulting peak profiles showed that anthocyanin profiles were altered during two growing seasons (Figure 3A).

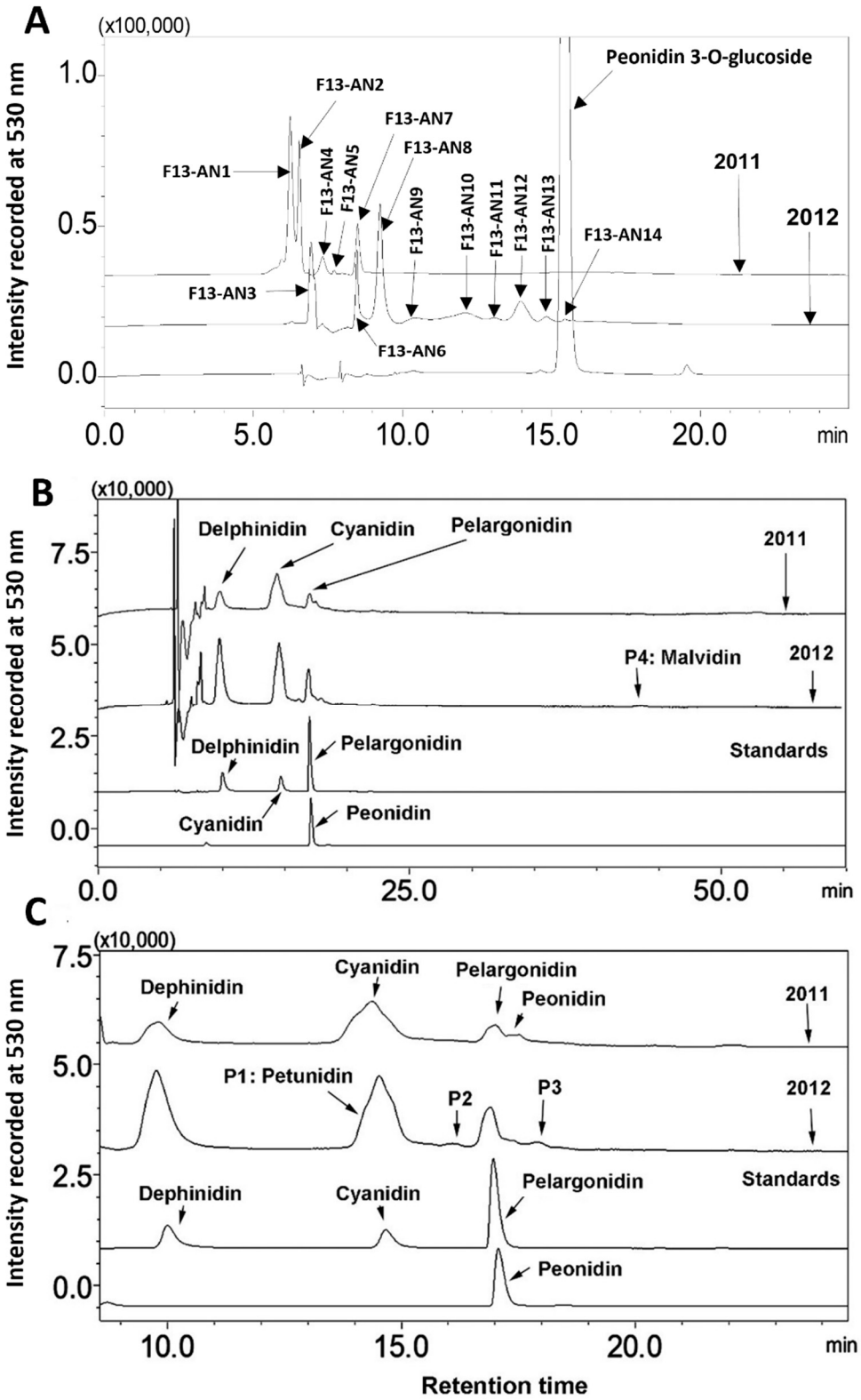

Figure 3. Comparison of anthocyanin and anthocyanidin profiles in berries of FLH 13-11 harvested in the 2011 and 2012 cropping seasons. (**A**) Comparison of anthocyanin profiles in berries from 2011 and 2012; (**B**) anthocyanidin profiles released from the hydrolysis of anthocyanins in 2011 and 2012; (**C**) four anthocyanidin standards.

Regardless of years, 14 anthocyanin peaks were detected from extracts of two seasons' berries. Based on retention times, these peaks were labeled as from F13-AN1 to F13-AN14

(Figure 3A). F13-AN1, 2, 4, 5, 6, and 7 were detected in berries harvested in 2011. Nine peaks, F13-AN3, 6, and 8–14, were detected in berries harvested in 2012. F13-AN6 was the only one detected in both years. These results revealed that the anthocyanin profiles in muscadine berries can be dramatically altered in two cropping seasons. This alteration most likely resulted from differences in weather in the two years. It is well understood that environmental factors can not only control anthocyanin production as discussed above but also can dramatically alter anthocyanin molecule complexity in the same plant. For example, *Arabidopsis thaliana* was reported to produce two anthocyanin molecules under regular growing conditions [27]. However, light condition changes can enhance the formation of nearly 30 anthocyanins in this model plant [20].

Anthocyanidin profiles. The different chromophores of anthocyanidins are the structural bases of anthocyanin hues. Butanol: HCl-based boiling was performed to completely hydrolyze anthocyanin extracts to release all anthocyanidins. HPLC-DAD-based profiling and HPLC-qTOF-MS/MS were performed to analyze anthocyanidins. The resulting data showed that anthocyanidin profiles were the same in berries from the two different years (Figure 3B). These data showed that although berries produced different anthocyanin profiles in two cropping seasons (Figure 3A), they biosynthesized the same anthocyanidins. Based on four authentic standards, delphinidin, cyanidin, pelargonidin, and peonidin, which were co-eluted as positive controls, the hydrolysis of anthocyanins produced four main peaks with the same retention times as these three core anthocyanidins (Figure 3C). In addition, four additional peaks were detected and labeled as P1, 2, 3, and 4 (Figure 3B,C).

HPLC-qTOF-MS analysis using the negative mode of ionization further showed that the primary mass-to-charge ratio values of the pelargonidin ($C_{15}H_{11}O_5^+$, molecular weight, MW, 271.24), cyanidin ($C_{15}H_{12}O_6^+$, MW, 287.24), delphinidin ($C_{15}H_{13}O_7^+$, MW, 303.24), and peonidin ($C_{16}H_{13}O_6^+$, MW, 301.24) standards were 269.265, 285.223, 301.213 [M − 2H], and 299. 213, respectively. Two ions were reduced from these standards in the negative mode. This ionization result was likely associated with the flavylium cation form of anthocyanidins in the acidic condition. In addition, second main m/z values for each standard were created by ESI. The m/z value (18) for each standard was added. Therefore, the second m/z values for the four standards were 287.265, 303.223, 319.213, and 317.213 $[M + 18 - 2H]^-$. Based on these MS features, berries produced all four of these anthocyanidins. In addition, there were four peaks detected at 530 nm, labeled as P1 through P4, (Figure 3B,C). P1 was shown as a shoulder together with cyanidin because the two were closely co-eluted. HPLC-qTOF-MS analysis revealed that the m/z values of P1 were 315.1347 [M − 2H] and 333.1347 [M + 18 − 2H]. The m/z values for P4 were 331.2968 [M − 2H] and 349.2968 [M + 18 − 2H]. Based on these mass spectra and retention times, P1 and P4 were annotated to be petunidin and malvidin, respectively. The m/z ratios of P2 and P3 were 365.1982 and 381.1314 [M − H], respectively. Their structures remain to be elucidated in the future.

HPLC-qTOF-MS/MS-based characterization of anthocyanins. HPLC-qTOF-MS/MS was performed to annotate anthocyanins detected in extracts of berries. Fourteen anthocyanins (Figure 3A) were ionized using the negative mode, and each anthocyanin ion was formed in the ion source. The resulting ions (primary ions) were separated by mass-to-charge ratio in the first stage of mass spectrometry (MS1). Each particular mass-to-charge ratio from each anthocyanin peak was selected to create fragment ions by collision-induced dissociation (CID). The resulting fragment ions (secondary ions) were separated and detected in a second stage of mass spectrometry (MS2). Primary and secondary ions generated for each anthocyanin peak were analyzed to annotate a structure.

To annotate anthocyanin peaks, the peonidin 3-glycoside (or glucoside) (Pn-3-G) standard was used as a reference to understand the main ion and CID features generated from our instrument. The molecular weight (MW) of Pn-3-G was 463.415. After ESI, its EIC was searched from total ion chromatographs (TICs). The resulting EIC and enhanced charge capacity (ECC) ion products showed that two primary m/z ratio values were 479.2307 and 461.1927 [M − 2H] (Figure 4A–C). The m/z ratio of 479.1927 was derived from 463.415 + 18 − 2H [M + 18 − 2H]. CID was performed to demonstrate the core structure in 479.1927

and 461.1927 $[m/z]^-$. CID analysis revealed that two typical fragments of 299.1927 and 163.0682 (Figure 4D,E) were generated from 479.2307 and 461.1927 $[m/z]^-$.

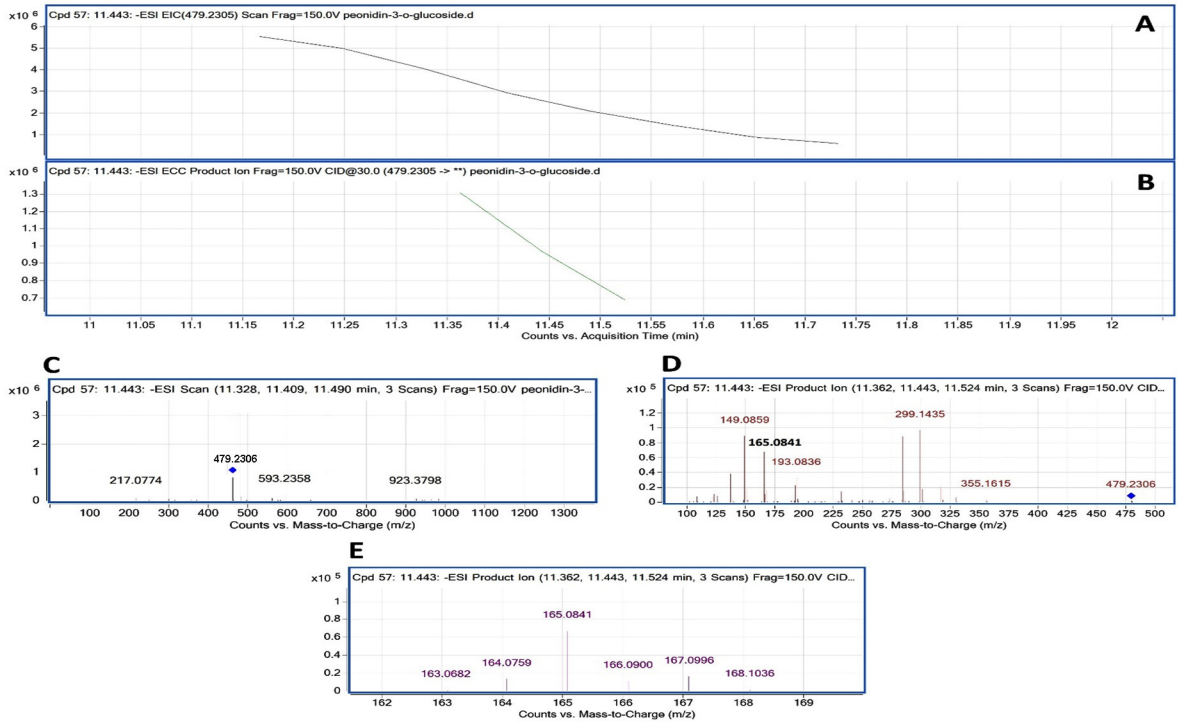

Figure 4. Extracted ion chromatogram (EIC) of primary mass spectrum (MS1) and m/z features of secondary ion fragments (MS2) derived from LC-MC/MS of peonidin 3-gluoside (Pn-3-G, molecular weight: 463.415) standard. (**A**) EIC of primary ion 479.2305 $[M + 18 - 2H]^-$, (**B**) enhanced charge capacity (ECC) ion product for 479.2305, (**C**) an MS profile showing two extracted m/z values, 461.1927 $[M - 2H]^-$ and 479.2307 $[M + 18 - 2H]^-$, (**D**,**E**) fragments from CID of 479.2307 and 461.1927 showing 299.1435 $[m/z]^-$ and 301.1927 $[m/z]^-$ relating to peonidin aglycone (**D**) and 161.0858–165.082 and 166.0858 relating to glucose (**E**). Blue "◊": the primary mass spectrum of the compound; "**": fragments derived from the primary mass spectrum. CID: collision induced disassociation. "peonidin-3": peonidin-3-glucoside. Cpd: compound database.

These ion fragments resulted from the homolytic dissociation of peonidin (299.1927) and the glucose group (163.0682) in both 461.1927 and 479.1927 $[m/z]^-$. In addition, fragments relating to peonidin observed from CID included 300.1927 and 301.1927. Fragments relating to glucose observed from CID consisted of 161.06 to 163.0682 and 165.0841 to 168.1036 (Figure 4E). These CID fragmentation profiles resulted from heterolytic fragmentation that has been commonly observed in MS/MS analysis [28–31]. All these data showed that in addition to an expected m/z ratio and homolytic fragmentations from the CID of Pn-3-G, other m/z ratios and heterolytic dissociation fragmentations were generated from this anthocyanin molecule. Based on these observations, anthocyanin peaks from berries were annotated in the following descriptions.

The peak F13-AN14 had the same retention time as Pn-3-G (Figure 3A). MS/MS generated its EIC m/z value and profiles of CID fragmentation. The resulting data showed that its m/z values and EIC were the same as those of Pn-3-G (Figure 5A–C). Its CID fragment profiles were also highly identical to those of Pn-3-G (Figure 5D,E). Based on these features, F13-AN14 was identified to be Pn-3-G (Figure 5F).

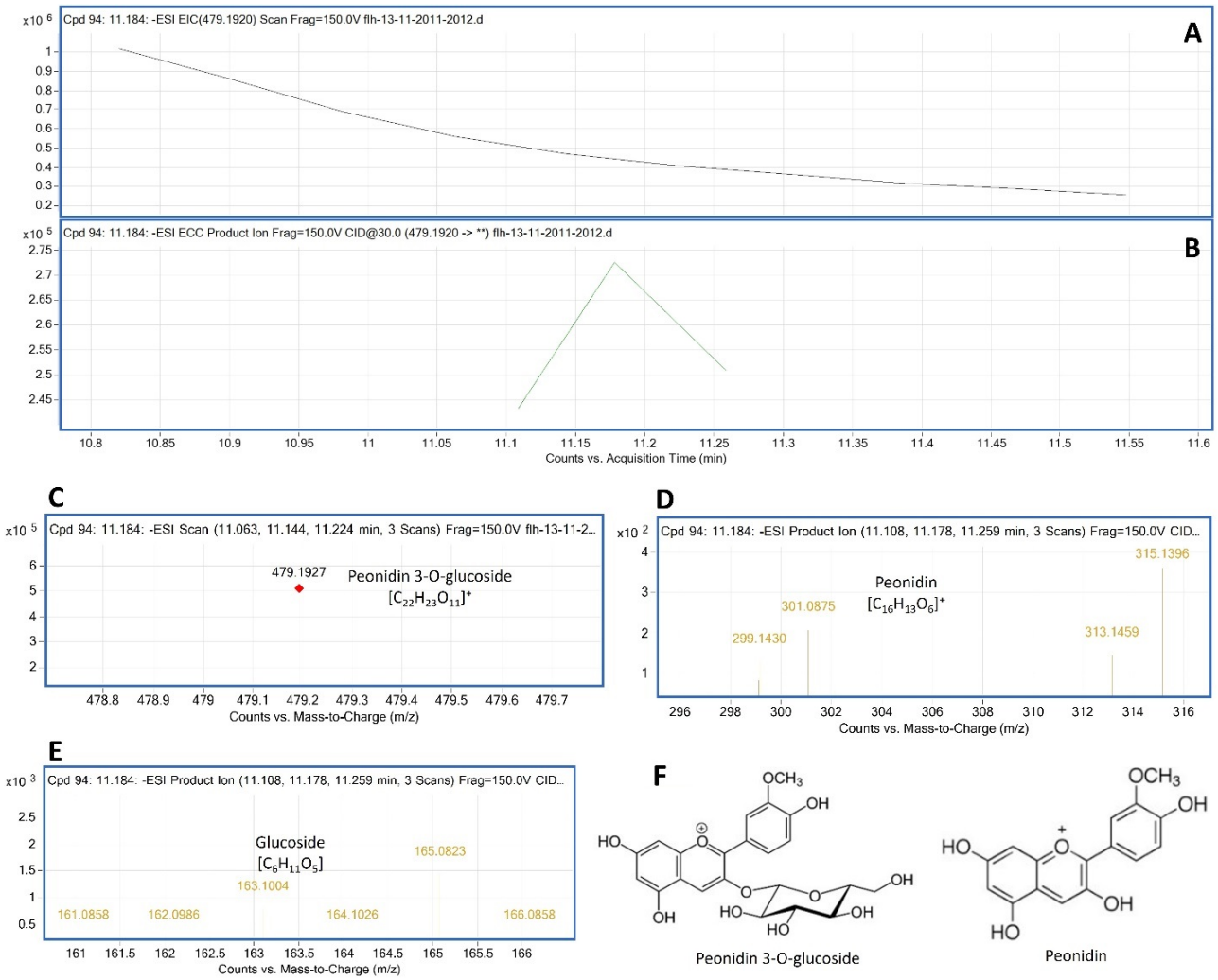

Figure 5. Extracted ion chromatogram (EIC) of primary mass spectrum and m/z features of secondary ion fragments derived from LC-MC/MS of peak F13-AN14. These data show this peak is peonidin 3-glucoside. (**A**) EIC of primary ion 479.2305 $[m/z]^-$, [M + 18 − 2H], (**B**) enhanced charge capacity (ECC) ion product for 479.2305, (**C**) an MS profile showing one extracted m/z value, 479.2307 $[m/z]^-$, (**D**,**E**) fragments from CID of 479.2307 showing 299.1435 $[m/z]$ and 301.1927 $[m/z]$ relating to peonidin aglycone (**D**), 161.0858–165.0823 and 166.0858 $[m/z]$ relating to glucose (**E**), and (**F**) structures of peonidin 3-glucoside and peonidin. Red "◊": the primary mass spectrum of the compound; "**": fragments derived from the primary mass spectrum. CID: collision induced disassociation. Cpd: compound database.

Delphinidin 3,5-diglucoside (Del-3,5-dG) is a common anthocyanin molecule in berries of muscadine. In our samples, F13-AN6 detected by HPLC-DAD was annotated to be Del-3,5-dG by LC-qTOF-MS/MS analysis. The MW of Del-3,5-dG was 627.5280. An MS search from TICs obtained two primary m/z values for this peak, 643.2822 [M + 18 − 2H] and 625.2822 [M − 2H], which were further demonstrated with its extracted EIC and EIC-ECC ion products (Figure 6A–C). CIDs of 625.2822 and 643.2822 generated five groups of secondary ion fragments (Table 1), group 1: 481.2083 [463.1951 + 18]; group 2: 463.1951 (Figure 6D); group 3: 301.0886 and 303.1268; group 4: 317.1254 and 319.1353 (Figure 6E); and group 5: 163.0963, 165.0832, 166.0824, 167.0988, and 168.1047 (Figure 6F).

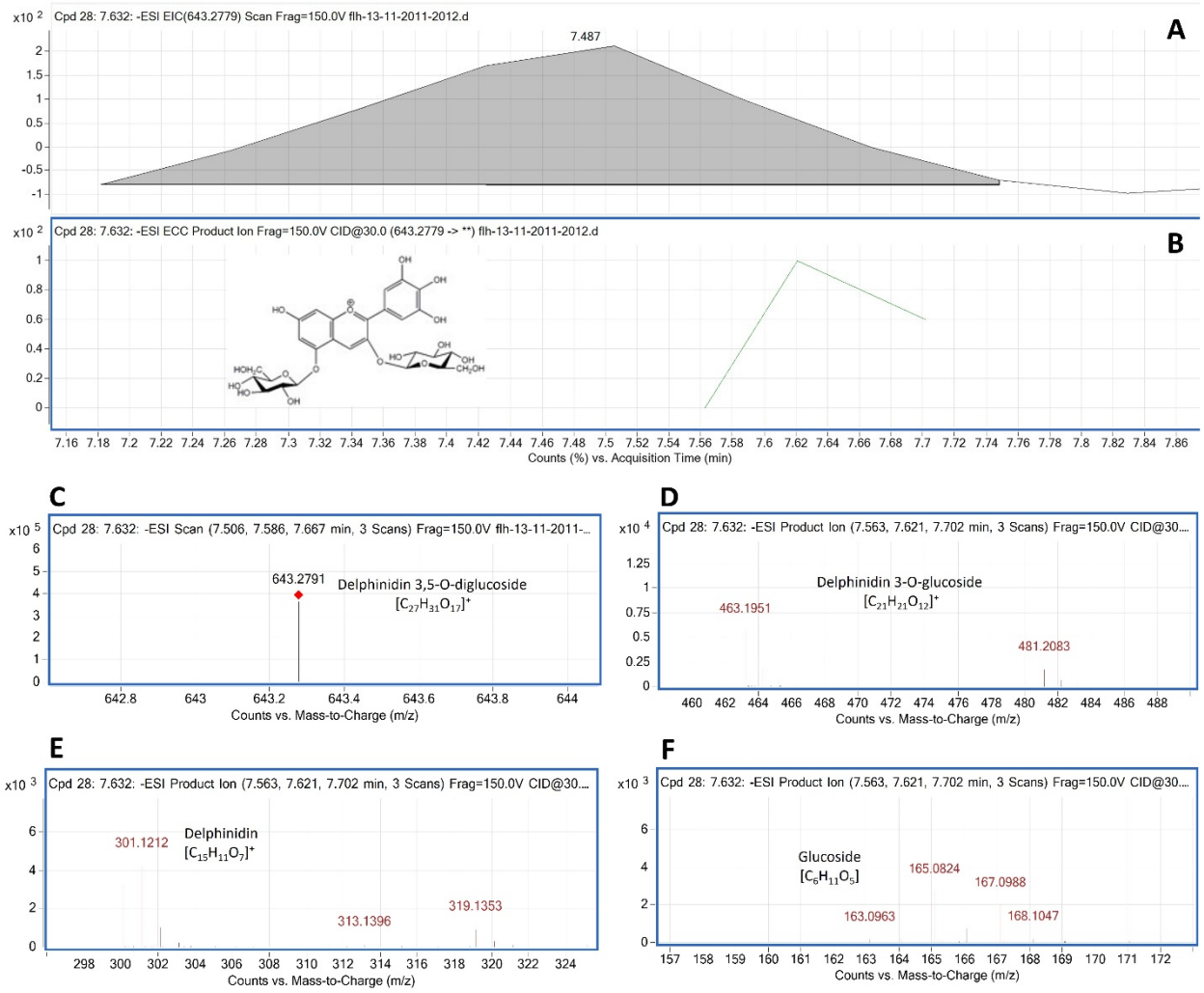

Figure 6. Extracted ion chromatogram (EIC) of primary mass spectrum and m/z features of secondary ion fragments derived from LC-MC/MS of peak F13-AN6. These data annotate this peak to be delphinidin 3, 5-digluoside (Del-3,5-dG, molecular weight: 427.528). (**A**) EIC of primary ion 643.2791 $[m/z]^-$, [M + 18 − 2H], (**B**) enhanced charge capacity (ECC) ion product for 643.2791 $[m/z]^-$, (**C**) an MS profile showing an extracted m/z value, 643.2791 $[m/z]^-$, [M + 18 − 2H], (**D**–**F**) fragments from CID of 643.2791 showing 463.1951 and 464.1953 $[m/z]^-$ relating to Del-3-G (**D**), 300.111, 301.1212, and 302.1213 $[m/z]^-$ relating to delphinidin aglycone (**E**), and 163.0963–168.1047 relating to glucose (**F**). Red "◊": the primary mass spectrum of the compound; "**": fragments derived from the primary mass spectrum. CID: collision induced disassociation. Cpd: compound database.

Based on these ion fragment features, the second group that resulted from the dissociation of the first glucose group (163.0686) from 625.2822 was relating to Del-3-glucoside. The third group that resulted from another dissociation of the second glucose group from 463.1951 was relating to delphinidin aglycone. The third group that resulted from the dissociation from 625.2822 and 464.2128–467.2174 was relating to glucose. Based on these features, this F13-AN13 peak was annotated to be Del-3,5-dG.

Cyanidin 3,5-diglucoside (Cy-3, 5-dG) is another common anthocyanin molecule formed in berries of different muscadine cultivars. Based on MS/MS data, F13-AN2 (Figure 3A) was annotated as Cy-3, 5-dG (Figure S1). After ESI, two primary m/z values of this peak were 609.529 $[M - 2H]^-$ and 627.529 $[M + 18 - 2H]^-$ (Figure S1A–C). CIDs of 609.529 and 627.529 generated fragments (Figure S1D–F), which were characterized by five groups of secondary m/z values (Table 1). Fragments 447.1979, 285.1244, and 163.0677 were related to Cy-3-G, cyanidin aglycone, and glucose.

Table 1. Mass spectrum characterization and annotation of 14 anthocyanin peaks by HPLC-qTOF-MS/MS analysis.

Peak #	λ (nm) and Rt (min)	MW and MS1 [*m*/*z*]$^-$	MS2 [*m*/*z*] Fragments from CID	Anthocyanin Annotation	Seasons (Figures)
F13-AN1	**λ:** 525 Rt: 6.258	MW: Unknown MS1: 643.2778	1. **481.2036**; 2. 463.1935, 465.1953; 3. **301.1211**–304.986; 4. 319.1345; 5. **163.0615**; 165.0822; 167.1998	Delphinidin 3,5-O-diglucoside-like anthocyanin	2011 Figure S4
F13-AN2	**λ:** 522 Rt: 6.269	MW: Unknown MS1: 679.2582	1. **447.1949**, 455.0124, 463.1942; 2. 283.1062–**285.1186**; 3. 301.1217–302.1217; 4. **163. 0826**, 165.0836–166.0834	Cyanidin 3,5-O-diglucoside-like anthocyanin	2011 Figure S5
F13-AN3	**λ:** 523 Rt: 7.163	MW: 465.3870 MS: 481.1751	1. **301.0852**–302.0852; 2. 317.3565; 3. **165.0864**, 167.0622, 168.0651	Delphinidin 3-O-glucoside-like anthocyanin	2012 Figure S6
F13-AN4	**λ:** 525 Rt: 7.238	MW: Unknown MS: 793.3089	1. **477.2128**, 481.2091, 482.2091, 495.2120; 2. **315.1352**, 319.14; 3. 329.1790, 331.1528; 4. **165.0829**	Petunidin 3,5-O-diglucoside-like anthocyanin	2011 Figure S7
F13-AN5	**λ:** 529 Rt: 7.310	MW: Unknown MS: 741.2607	1. 481.2082, 482.2082; 2. **463.1966**, 464.2045; 3. 297.0398, 299.0396, **301.1168**; 4. 317.1776, 319.1397; 5. 162.1067, 165.0836, 167.0892	Delphinidin 3,5-O-diglucoside-like anthocyanin	2011 Figure S8
F13-AN6	**λ:** 523 Rt: 7.632	MW: 627.5280 MS1: 643.2791	1. 481.2083; 2. **463.1951**; 3. **301.0886**, 303.1268; 4. 317.1254, **319.1353**; 5. **163.0963**, 165.0832, 166.0824, 167.0988, 168.1047	Delphinidin 3,5-O-diglucoside	2011, 2012 Figure 6
F13-AN7	**λ:** 517 Rt: 8.285	MW: 611.5290 MS1: 627.2824	1. 465.2126; 466.2126; 2. **447.1979**, 448.1979; 3. **285.1244**, 287.1318; 4. 301.0886, 303.1381; 5. **163.0677**, 164.0716, 165.0832, 166.0919	Cyanidin 3,5-O-diglucoside	2011 Figure S1
F13-AN8	**λ:** 520 Rt: 8.371	MW: 641.2820 MS1: 657.2963	1. 495.2253, 496.2263; 2. **477.2127**, 478.2127; 3. 327.1626, 329.1787, 331.1731, 333.1531; 4. 314. 1392, **315.1392**, 317.1399; 5. **163.0843**, 165.0822, 167.0933, 169.0802	Petunidin 3,5-O-diglucoside	2012 Figure S2
F13-AN9	**λ:** 514 Rt: 9.988	MW: Unknown MS1: 493.2101	1. 330.1279, 331.1153, 332.1253; 2. 315.1028, 316.1028, 317.1058; 3. 298.1063, **299.1063**, 301.110; 4. **163.0836**, 165.0836, 166.0824, 167.0988	Peonidin-3-O-glucoside-like anthocyanin	2012 Figure S9
F13-AN10	**λ:** 523 Rt:10.462	MW: 625.5560 MS1: 641.2635	1. **461.1782**, 479.1915; 2. 315.1414, 317.1224; 3. **299.1090**, 301.1226; 4. **163.1029**, 165.0835, 166.0863	Peonidin 3,5-O-diglucoside	2012 Figure S3

Table 1. *Cont.*

Peak #	λ (nm) and Rt (min)	MW and MS1 [*m*/*z*]$^-$	MS2 [*m*/*z*] Fragments from CID	Anthocyanin Annotation	Seasons (Figures)
F13-AN11	**λ:** 523 Rt: 0.693	MW: Unknown MS1: 633.1995	1. 481.1651; 2. **463.1594**, 464.1745, 465.1745, 466.1779; 3. 300.0765, **301.0857**, 302.0890, 303.0909; 4. 161.0926, **163.1045**, 165.0810, 167.0624	Delphinidin 3,5-O-diglucoside-like anthocyanin	2012 Figure S10
F13-AN12	**λ:** 518 Rt:11.028	MW: Unknown MS1: 453.1748	1. **271.1062**, 272.1154, 273.1232, 274.1285; 2. **163.1029**, 165.0829, 166.0863	Pelargonidin 3-O-glucoside-like anthocyanin	2012 Figure S11
F13-AN13	**λ:** 524 Rt: 1.039	MW: 655.587 MS1: 673.2911	1. **493.2083**, 494.2080, 495.2101; 2. 330.1328, **331.1448**, 332.1328; 3. 161.1010, **163.0708**, 165.0829, 166.0869	Malvidin 3,5-O-diglucoside	2012 Figure S12
F13-AN14	**λ:** 529 Rt: 1.184	MW: 463.4150 MS1: 479.1927	1. 313.1459, 315.1396 2. **299.1430**, 301.0875; 3. 161.0858, **163.0709**, 165.082, 166.0858	Peonidin 3-O-glucoside	2012 Figure 5

Note: numbers highlighted by bold letters show those fragments resulted from homolytic fragmentations of collision-induced dissociation (CID).

Accordingly, based on MS1 and MS2 generated from MS/MS analysis, 11 additional peaks were annotated to either a known anthocyanin or characterized to be a specific anthocyanidin-related anthocyanin molecule (Table 1, Figures S2–S12). Based on anthocyanin molecules reported in the muscadine literature [9,11,14,15,17,19], the common five 3,5-diglucosides of anthocyanidins were found from anthocyanin extracts (Table 1). Furthermore, this analysis identified four monoglucosides of anthocyanidins. Three were peonidin 3-glucoside, pelargonidin 3-glucoside-like, and malvidin 3-glucoside-like anthocyanins that were only detected in 2012, while one was delphinidin-3 glucoside-like anthocyanin that was only detected in 2011. These results indicate that the anthocyanin profiles in berries of FLH 13-11 are closely associated with the cropping seasons.

4. Conclusions

Muscadine products such as wines and juices have a poor color stability problem. This problem is associated with anthocyanin structures lacking monoglucoside. In addition, whether cropping seasons can alter anthocyanin structure profiles in muscadine berries remains unknown. To understand these two problems, the high-performance liquid chromatography–diode array detector (HPLC-DAD) and HPLC–quadrupole time-of-flight tandem mass spectrometer (HPLC-qTOF-MS/MS) approaches were used to perform metabolic profiling and annotation of anthocyanins and anthocyanidins in ripe berries from two continuous cropping seasons. In particular, protocols of HPLC-qTOF-MS/MS were developed to annotate anthocyanin structures.

Metabolic profiling showed that two cropping seasons significantly altered anthocyanin productions, profiles, and structures in a hybrid muscadine variety, FLH 13-11. Fourteen anthocyanins were detected from two years of berries. Six and nine were produced in the first and second season, respectively. However, only one anthocyanin was produced in two years' berries. More importantly, in addition to known anthocyanidin-diglucosides, three anthocyanidin-monoglucosides, including one known peonidin 3-glycoside and two unknowns, were discovered in the second season but not in the first season. These results show that anthocyanins of FLH 13-11 are controlled by cropping seasons and this hybrid is an elite variety to produce anthocyanidin-monoglucoside for color stability.

This discovery is informative for muscadine agriculture and the industry for stable and high-quality color products. The regulation of anthocyanin structures by cropping seasons shows that it is necessary to analyze anthocyanin structures in berries to predict color stability in wine and juice products. The discovery of anthocyanidin-monoglucosides in the second season not only demonstrates that FLH 13-11 is an elite hybrid for new muscadine anthocyanin structures but also shows muscadine industries that field conditions during cropping seasons are essentially associated with anthocyanin structures.

Supplementary Materials: The following supporting information can be downloaded at: https://www.mdpi.com/article/10.3390/agronomy14030442/s1. Figure S1: Extracted ion chromatogram (EIC) of primary mass spectrum and m/z features of secondary ion fragments derived from LC-MC/MS of peak F13-AN7. Figure S2: Extracted ion chromatogram (EIC) of primary mass spectrum and m/z features of secondary ion fragments derived from LC-MC/MS of peak F13-AN8. Figure S3: Extracted ion chromatogram (EIC) of primary mass spectrum and m/z features of secondary ion fragments derived from LC-MC/MS of peak F13-AN10. Figure S4: Extracted ion chromatogram (EIC) of primary mass spectrum and m/z features of secondary ion fragments derived from LC-MC/MS of peak F13-AN1. Figure S5: Extracted ion chromatogram (EIC) of primary mass spectrum and m/z features of secondary ion fragments derived from LC-MC/MS of peak F13-AN2. Figure S6: Extracted ion chromatogram (EIC) of primary mass spectrum and m/z features of secondary ion fragments derived from LC-MC/MS of peak F13-AN3. Figure S7: Extracted ion chromatogram (EIC) of primary mass spectrum and m/z features of secondary ion fragments derived from LC-MC/MS of peak F13-AN4. Figure S8: Extracted ion chromatogram (EIC) of primary mass spectrum and m/z features of secondary ion fragments derived from LC-MC/MS of peak F13-AN5. Figure S9: Extracted ion chromatogram (EIC) of primary mass spectrum and m/z features of secondary ion fragments derived from LC-MC/MS of peak F13-AN9. Figure S10: Extracted ion chromatogram (EIC) of primary mass spectrum and m/z features of secondary ion fragments derived from LC-MC/MS of peak F13-AN11. Figure S11: Extracted ion chromatogram (EIC) of primary mass spectrum and m/z features of secondary ion fragments derived from LC-MC/MS of peak F13-AN12. Figure S12: Extracted ion chromatogram (EIC) of primary mass spectrum and m/z features of secondary ion fragments derived from LC-MC/MS of peak F13-AN13. Figure S13: Annual average high and maximum highest temperatures for Wilmington in 2011 and 2012. Figure S14: Annual average high and maximum highest temperatures for Castle Hayne in 2011 and 2012.

Author Contributions: Conceptualization, D.-Y.X.; funding acquisition, J.B.; investigation, S.Y. and G.L.; methodology, S.Y. and D.-Y.X.; project administration, D.-Y.X.; resources, J.B.; supervision, J.B. and D.-Y.X.; writing—original draft, S.Y. and G.L.; writing—review and editing, S.Y. and D.-Y.X. All authors have read and agreed to the published version of the manuscript.

Funding: This research was funded by the North Carolina State University for Plant Breeding.

Data Availability Statement: Data are contained within the article and Supplementary Materials.

Acknowledgments: Grape research station provided samples for this investigation.

Conflicts of Interest: The authors declare no conflicts of interest.

References

1. Brown, W.L. The Anthocyanin Pigment of the Hunt Muscadine Grape. *J. Am. Chem. Soc.* **1940**, *62*, 2808–2810. [CrossRef]
2. Olien, W.C. Introduction to the Muscadines. In *Muacadine Grapes*; Basiouny, F.M., Himelrick, D.G., Eds.; ASHA Press: Alexandria, VA, USA, 2001; pp. 1–13.
3. Mortensen, J.A. Cultivars. In *Muscadine Grapes*; Basiounny, F.M., Himelrick, D.G., Eds.; ASHA Press: Alexandria, VA, USA, 2001; pp. 91–105.
4. You, Q.; Chen, F.; Wang, X.; Luo, P.G.; Jiang, Y. Inhibitory effects of muscadine anthocyanins on alpha-glucosidase and pancreatic lipase activities. *J. Agric. Food Chem.* **2011**, *59*, 9506–9511. [CrossRef] [PubMed]
5. Gourineni, V.; Shay, N.F.; Chung, S.; Sandhu, A.K.; Gu, L. Muscadine grape (*Vitis rotundifolia*) and wine phytochemicals prevented obesity-associated metabolic complications in C57BL/6J Mice. *J. Agric. Food Chem.* **2012**, *60*, 7674–7681. [CrossRef] [PubMed]
6. Wang, X.; Tong, H.; Chen, F.; Gangemi, J.D. Chemical characterization and antioxidant evaluation of muscadine grape pomace extract. *Food Chem.* **2010**, *123*, 1156–1162. [CrossRef]
7. Striegler, R.; Morris, J.; Carter, P.; Clark, J.; Threlfall, R.; Howard, L. Yield, quality, and nutraceutical potential of selected muscadine cultivars grown in southwestern Arkansas. *HortTechnology* **2005**, *15*, 276–284. [CrossRef]

8. Goldy, R.; Ballinger, W.; Maness, E.; Swallow, W. Anthocyanin content of fruit, stem, tendril, leaf, and leaf petioles in muscadine grape. *J. Am. Soc. Hortic. Sci.* **1987**, *112*, 880–882. [CrossRef]
9. Nesbitt, W.B.; Maness, E.P.; Ballinger, W.E.; Carroll, D.E. Relationship of anthocyanins of black muscadine grapes (*Vitis rotundifolia* Michx) to wine color. *Am. J. Enol. Vitic.* **1974**, *25*, 30–32. [CrossRef]
10. Cardona, J.A.; Lee, J.-H.; Talcott, S.T. Color and polyphenolic stability in extracts produced from muscadine grape (*Vitis rotundifolia*) pomace. *J. Agric. Food Chem.* **2009**, *57*, 8421–8425. [CrossRef]
11. You, Q.; Chen, F.; Wang, X.; Sharp, J.L.; You, Y. Analysis of phenolic composition of Noble muscadine (*Vitis rotundifolia*) by HPLC-MS and the relationship to its antioxidant capacity. *J. Food Sci.* **2012**, *77*, C1115–C1123. [CrossRef]
12. Conner, P.J.; MacLean, D. Fruit anthocyanin profile and berry color of muscadine grape cultivars and muscadinia germplasm. *HortScience* **2013**, *48*, 1235–1240. [CrossRef]
13. Barchenger, D.W.; Clark, J.R.; Threlfall, R.T.; Howard, L.R.; Brownmiller, C.R. Evaluation of physicochemical and storability attributes of muscadine grapes (*Vitis rotundifolia* Michx.). *HortScience* **2015**, *50*, 104–111. [CrossRef]
14. You, Q.; Chen, F.; Sharp, J.L.; Wang, X.; You, Y.; Zhang, C. High-performance liquid chromatography–mass spectrometry and evaporative light-scattering detector to compare phenolic profiles of muscadine grapes. *J. Chromatogr. A* **2012**, *1240*, 96–103. [CrossRef] [PubMed]
15. Yuzuak, S.; Xie, D.-Y. Anthocyanins from muscadine (*Vitis rotundifolia*) grape fruit. *Curr. Plant Biol.* **2022**, *30*, 100243. [CrossRef]
16. Goldy, R.G.; Maness, E.P.; Stiles, H.D.; Clark, J.R.; Wilson, M.A. Pigment quantity and quality characteristics of some native *Vitis rotundifolia* Michx. *Am. J. Enol. Vitic.* **1989**, *40*, 253–258. [CrossRef]
17. Lamikanra, O. Anthocyanins of *Vitis rotundifolia* hybrid grapes. *Food Chem.* **1989**, *33*, 225–237. [CrossRef]
18. Goldy, R.G.; Ballinger, W.E.; Maness, E.P. Fruit anthocyanin content of some Euvitis × *Vitis rotundifolia* hybrids. *J. Am. Soc. Hortic. Sci.* **1986**, *111*, 955–960. [CrossRef]
19. Ballinger, W.E.; Maness, E.P.; Nesbitt, W.B.; Carroll, D.E. Anthocyanins of black grapes of 10 clones of Vitis rotundifolia, MICHX. *J. Food Sci.* **1973**, *38*, 909–910. [CrossRef]
20. Shi, M.-Z.; Xie, D.-Y. Features of anthocyanin biosynthesis in pap1-D and wild-type Arabidopsis thaliana plants grown in different light intensity and culture media conditions. *Planta* **2010**, *231*, 1385–1400. [CrossRef]
21. Zhou, L.L.; Zeng, H.N.; Shi, M.Z.; Xie, D.Y. Development of tobacco callus cultures over expressing Arabidopsis PAP1/MYB75 transcription factor and characterization of anthocyanin biosynthesis. *Planta* **2008**, *229*, 37–51. [CrossRef]
22. He, X.; Li, Y.; Lawson, D.; Xie, D.Y. Metabolic engineering of anthocyanins in dark tobacco varieties. *Physiol. Plant.* **2017**, *159*, 2–12. [CrossRef]
23. Albert, N.W.; Lewis, D.H.; Zhang, H.; Irving, L.J.; Jameson, P.E.; Davies, K.M. Light-induced vegetative anthocyanin pigmentation in Petunia. *J. Exp. Bot.* **2009**, *60*, 2191–2202. [CrossRef] [PubMed]
24. Matus, J.T.; Loyola, R.; Vega, A.; Peña-Neira, A.; Bordeu, E.; Arce-Johnson, P.; Alcalde, J.A. Post-veraison sunlight exposure induces MYB-mediated transcriptional regulation of anthocyanin and flavonol synthesis in berry skins of Vitis vinifera. *J. Exp. Bot.* **2009**, *60*, 853–867. [CrossRef] [PubMed]
25. Cominelli, E.; Gusmaroli, G.; Allegra, D.; Galbiati, M.; Wade, H.K.; Jenkins, G.I.; Tonelli, C. Expression analysis of anthocyanin regulatory genes in response to different light qualities in Arabidopsis thaliana. *J. Plant Physiol.* **2008**, *165*, 886–894. [CrossRef] [PubMed]
26. Rowan, D.D.; Cao, M.; Lin-Wang, K.; Cooney, J.M.; Jensen, D.J.; Austin, P.T.; Hunt, M.B.; Norling, C.; Hellens, R.P.; Schaffer, R.J.; et al. Environmental regulation of leaf colour in red *35S:PAP1 Arabidopsis thaliana*. *New Phytol.* **2009**, *182*, 102–115. [CrossRef] [PubMed]
27. Bloor, S.J.; Abrahams, S. The structure of the major anthocyanin in Arabidopsis thaliana. *Phytochemistry* **2001**, *59*, 343–346. [CrossRef] [PubMed]
28. Geng, P.; Sun, J.; Zhang, R.; He, J.; Abliz, Z. An investigation of the fragmentation differences of isomeric flavonol-*O*-glycosides under different collision-induced dissociation based mass spectrometry. *Rapid Commun. Mass Spectrom.* **2009**, *23*, 1519–1524. [CrossRef] [PubMed]
29. Es-Safi, N.E.; Kerhoas, L.; Ducrot, P.H. Application of positive and negative electrospray ionization, collision-induced dissociation and tandem mass spectrometry to a study of the fragmentation of 6-hydroxyluteolin 7-O-glucoside and 7-O-glucosyl-(l -> 3)-glucoside. *Rapid Commun. Mass. Spectrom.* **2005**, *19*, 2734–2742. [CrossRef] [PubMed]
30. Yang, W.-Z.; Ye, M.; Qiao, X.; Wang, Q.; Bo, T.; Guo, D.-A. Collision-induced dissociation of 40 flavonoid aglycones and differentiation of the common flavonoid subtypes using electrospray ionization ion-trap tandem mass spectrometry and quadrupole time-of-flight mass spectrometry. *Eur. J. Mass Spectrom.* **2012**, *18*, 493–503. [CrossRef]
31. Ilboudo, O.; Tapsoba, I.; Bonzi-Coulibaly, Y.L.; Gerbaux, P. Targeting structural motifs of flavonoid diglycosides using collision-induced dissociation experiments on flavonoid/Pb^{2+} complexes. *Eur. J. Mass Spectrom.* **2012**, *18*, 465–473. [CrossRef]